energies

MDPI

Article

Influence of an Integral Heave Plate on the Dynamic Response of Floating Offshore Wind Turbine Under Operational and Storm Conditions

Yichen Jiang [1,2], Guanqing Hu [1], Zhi Zong [1,2,3,*], Li Zou [1,2,3] and Guoqing Jin [1]

[1] School of Naval Architecture, Dalian University of Technology, Dalian 116024, China; ycjiang@dlut.edu.cn (Y.J.); jxtx71045@mail.dlut.edu.cn (G.H.); lizou@dlut.edu.cn (L.Z.); jinguoqing2012@mail.dlut.edu.cn (G.J.)

[2] Collaborative Innovation Center for Advanced Ship and Deep-Sea Exploration, Shanghai 200240, China

[3] State Key Laboratory of Structural Analysis for Industrial Equipment, Dalian University of Technology, Dalian 116024, China

* Correspondence: zongzhi@dlut.edu.cn

Received: 18 August 2020; Accepted: 18 November 2020; Published: 22 November 2020

Abstract: The hydrodynamic performance of the floating foundation for offshore wind turbines is essential to its stability and energy harvesting. A semi-submersible platform with an integral heave plate is proposed in order to reduce the vertical motion responses. In this study, we compare the heave, pitch, and roll free decay motions of the new platform with a WindFloat-type platform based on Reynolds-Averaged Navier-Stokes simulations. The differences of the linear and quadratic damping properties between these platforms are revealed. Then, a FAST (Fatigue, Aerodynamics, Structures, and Turbulence) model with the consideration of fluid viscosity effects is set up to investigate the performance of the new platform under storm and operational conditions. The time-domain responses, motion spectra, and the mooring-tension statistics of these two platforms are evaluated. It is found that the integral heave plate can increase the viscous hydrodynamic damping, significantly decrease the heave and pitch motion responses, and increase the safety of the mooring cables, especially for the storm condition.

Keywords: offshore wind energy; floating offshore wind turbine; hydrodynamic performance; integral damping plate; FAST

1. Introduction

With environmental pollution worsening and rise in depletion of non-renewable energy, clean and environmental renewable energies are of wide concern. Owing to environmentally friendly, non-polluting, and inexhaustible features, wind power generation has become the fastest growing power generation in recent years [1]. From land to sea, from shallow to deep, and from fixed foundation to floating platforms; there have been inevitable development trends in wind farms [2]. However, one of the largest challenges to the structural design of a Floating Offshore Wind Turbine (FOWT) [3] is constraining its dynamic response within certain ranges to maintain sustainability and stability, under the combined excitation of wind and waves, especially under extreme sea conditions.

A heave plate, which can generate added mass and damping effects on the floating platform, is an effective device for limiting motions in the vertical plane [4]. There has been a fair bit of research on heave plates. Phillip et al. examined the effects of a circular heave plate on a spar platform [5]. Their results demonstrated that the added mass and viscous damping of the heave plate are key factors reducing the motion response of a floating platform. Then, Han et al. discussed the effect of the width and thickness of the damping plate on the heave, roll, and pitch damping of the semisubmersible

platform at different initial decay positions [6]. The effect mechanism of the heave plate was analyzed from a flow field perspective. It was found that during the motion of the heave plate, a vortex was induced at the edge, and flow separation occurs, which increased the motion damping and reduced the motion amplitude. Ding et al. investigated the effects of different structural parameters of heave plates, including plate number, shape, thickness etc., on its own hydrodynamic characteristics [7]. An and Faltinsen numerically performed the heave added mass and damping of horizontally submerged and perforated rectangular plates [8]. The effects of the perforation ratio, plate submergence, forcing period, and heave amplitude (KC number) were studied. In terms of experimental studies such as the free decay oscillation method or the forced oscillation method, Tao et al. revealed that the disk with 20% porosity yields approximately 30% increase in damping compared to the solid disk at f = 0.1 Hz and KC = 0.2, using model scale experiments [9]. In addition, forced oscillation tests on a single triangular plate arrangement and double-plate arrangement were carried out by Ji et al. [10]. The effects of space between the two plates on hydrodynamic coefficients were discussed, and the best gap was obtained.

One of the main characters of the FOWT system is that it suffers much larger aerodynamic loads compared to other offshore floating platforms. Evaluating the hydrodynamic performance of the FOWT system needs to consider the coupled effects between the aerodynamic loads and hydrodynamic loads. At present, an effective method used to investigate the dynamic response of FOWT is CFD simulation, which can directly include all related physical effects (flow viscosity, hydrostatic, wave diffraction, radiation, wave run-up, slamming, etc.) of the floating platform [11]. The other is a combination of NREL FAST, which has a mature aerodynamic load solving model, and the diffraction/radiation panel program, such as WAMIT [12], AQWA, WADAM, NEMOH, etc., which provide the hydrodynamic coefficient of the target platform. Li et al. used a combinational method of NREL FAST, and WADAM to study hydrodynamic modelling for an offshore wind turbine, with emphasis on the computation of second-order difference-frequency wave forces and their effects on the global rigid-body motion response [13].

Though several studies take into account the effect of the heave plate on hydrodynamics and the variational aerodynamic loads on rotor while simulating the dynamic response of the FOWT system, they mainly focus on the traditional oil and gas Spar platform, the load characteristic of which is quite different from that of the FOWT semi-submersible platform. Therefore, this paper presents a comparison of hydrodynamic performance between a semi-submersible WindFloat-type platform and the new one, HexaSemi, which has an integral heave plate, rather than WindFloat's three independent heave plates in combination with CFD, WADAM, and FAST. At first, the heave, pitch, and roll-decay motion of the two platforms are simulated in the way of STAR-CCM+ to account for the viscous effects of the heave plate. Then, we obtain their hydrodynamic coefficients by using the potential-theory based model, WADAM. Based on the decay motion time histories, the additional linear and quadratic damping coefficients of the above three degrees of freedom are obtained and implemented in the FAST model. Next, case studies with the input of operational and storm conditions are performed [14]. In the end, a comparison of the results of the HexaSemi and WindFloat-type platform is made to assess the performance and feasibility of the new proposed integral heave plate.

2. Numerical Models

The present study is mainly based on three numerical tools: WADAM, STAR-CCM+, and open-source FAST to develop the aerodynamic-hydrodynamic coupled analysis. The numerical simulation procedure is shown in Figure 1. The hydrodynamic analysis in the frequency domain is conducted by WADAM. A MATLAB program is compiled to read the WADAM output files and generate the input files for FAST HydroDyn module. In order to obtain the additional linear and quadratic damping coefficients for FAST and imitate all the important physics, the comparison for free-decay response analyses are carried out, using the advanced STAR-CCM+ software, which can provide accurate hydrodynamic responses without adjusting parameters. Then, FAST simulates 6-DOFs motion responses of the WindFloat-type platform and HexaSemi wind turbine systems under

wind-wave excitation, including an operational condition and a storm condition [15]. In the end, the post-processing analysis including motion response time history, spectrum, and a significant height was conducted by MATLAB to comprehensively compare the performance of the two platforms. Overall, Figure 1 illustrates the whole numerical simulation procedure.

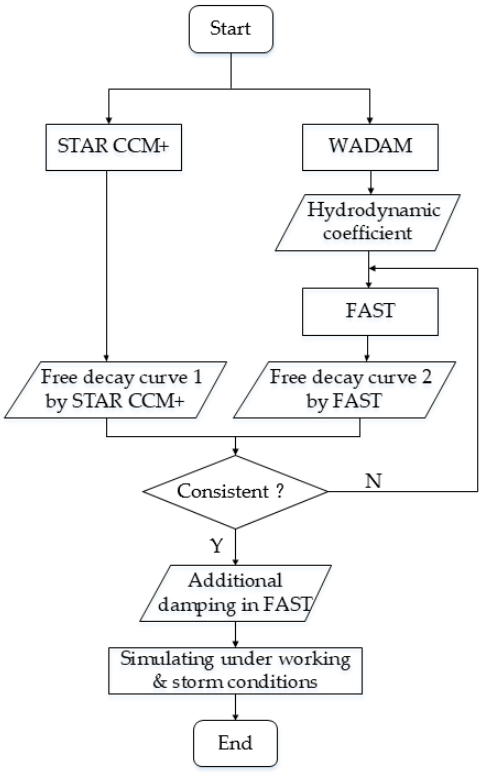

Figure 1. Numerical simulation procedure.

2.1. CFD Model (STAR-CCM+)

Numerical simulations of the heave, pitch, and roll-decay motion of the WindFloat-type platform and HexaSemi have been analyzed using the STAR-CCM+ software with an implicit unsteady method, overset grid technique, the trimmed cell mesh technique, VOF model and dynamic fluid body interaction (DFBI) module, in order to account for the viscous effects of the heave plate [16]. A segregated flow model is employed to solve the flow equations and the CFD simulation uses a realizable k-ε turbulence solver for all subsequent calculations. Figure 2 shows the whole fluid domain, mesh distribution, and boundary conditions established in this study.

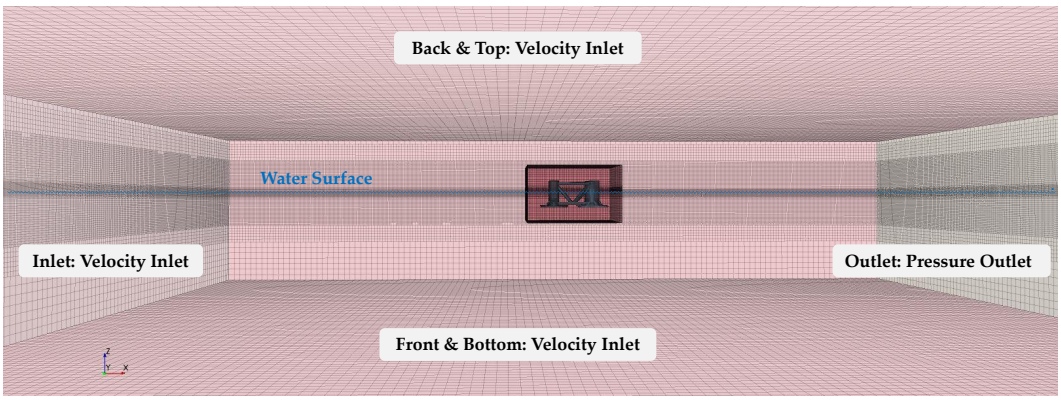

(**a**)

Figure 2. *Cont.*

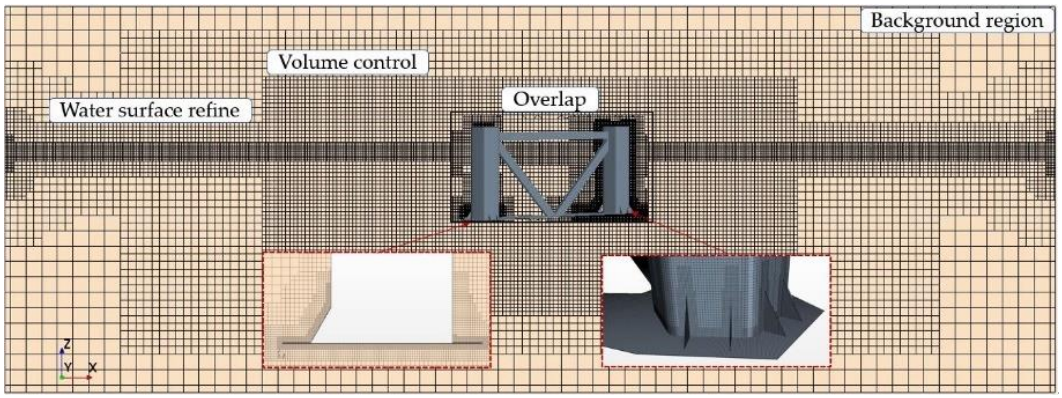

(**b**)

Figure 2. The whole fluid domain: (**a**) Boundary conditions in CFD, (**b**) Mesh distribution in xz-plane and close-up view of mesh around heave plate.

Additionally, it is necessary to create an overset interface between the two regions and assign the overset mesh type. The pre-processor of the CFD model uses automatic meshing operation and trimmed cell mesher for grids generation. The scale of the simulated platforms is large, so the y+ value of the realizable k-ε turbulence solver is relatively large, about 30~200. According to the selected y+ value, the thickness of the first prismatic layer can be obtained, and it is 3.39 mm. In order to reduce the number of grids, the factor of the layer stretching is set to be slightly larger (1.4). After four layers placed near the wall of foundation, the size of the outermost prismatic layer (0.0093 m) is approximately 25% of the size of the closest cell (0.045 m), which satisfies the requirement of good mesh size transition. In this case, the total boundary layer thickness is 0.024 m and the wall-cell y+ values around the surface of platform is about 30~200. As for the overlap region, the base size is 0.75 m. From the boundary of overlap region to the closest cell around the platform surface, there are eight transitional grid layers. Moreover, the thickness of the grid around the water surface is 0.375 m. At last, the total number of cells is 6.97 million for the WindFloat-type platform model and 7.84 million for HexaSemi.

The CFD simulation model uses a realizable k-ε turbulence solver in all calculations, which belongs to the RANS turbulent model. The time-step scheme adopt implicit unsteady model and time step is 0.02 s. The maximum inner iteration is 10 in each time step. The Volume of Fluid method is used to solve the multiphase flows involving free surface at the air-water interface and capture the free water surface. The simulation was done by a customized desktop computer with an 8-core Ryzen 7 1800X processor (3.6 GHz) and 32 Gb RAM. It took 120 h for simulating four periods of the heave decay motion, approximately.

2.2. WADAM

The WADAM, called Wave Analysis by Diffraction and Morison Theory, is a general hydrodynamic analysis program based on diffraction theory and Morison theory for calculating wave-structure interaction for fixed and floating structures of arbitrary shape. Airy wave theory is applied and results are presented as complex transfer functions or as deterministic results for specified phases of the wave. In the calculation of wave load, it uses three-dimensional radiation-diffraction theory for large scale structures and uses the Morison equation for the slender structure (DNV, 2008). The hydrodynamic coefficients of the WindFloat-type platform and HexaSemi are obtained by using WADAM in this study. Figure 3 describes the WADAM models.

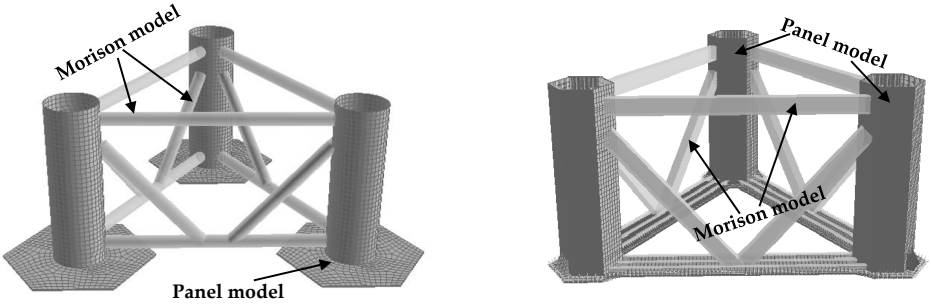

(**a**) (**b**)

Figure 3. (**a**) WindFloat-type platform and (**b**) HexaSemi WADAM models.

During the analysis in frequency domain, the wave propagates at 0 degree, and the frequency range is from 1 Hz to 40 Hz with the equal frequency interval of 1 Hz. Figure 4 shows the comparisons of hydrodynamic coefficients in all 6 DOFs.

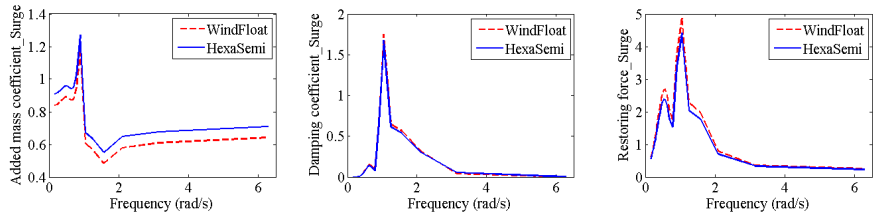

(**a**)

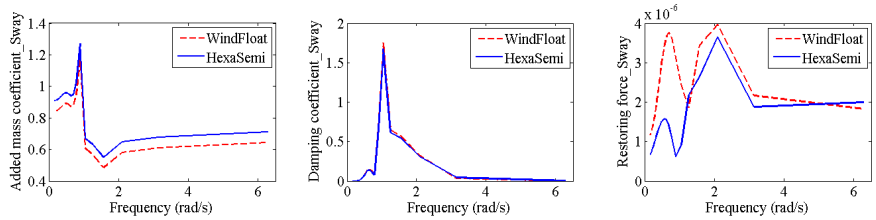

(**b**)

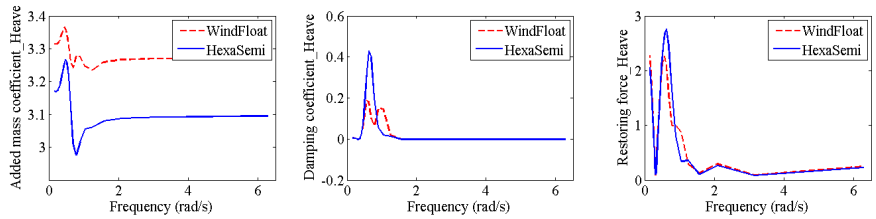

(**c**)

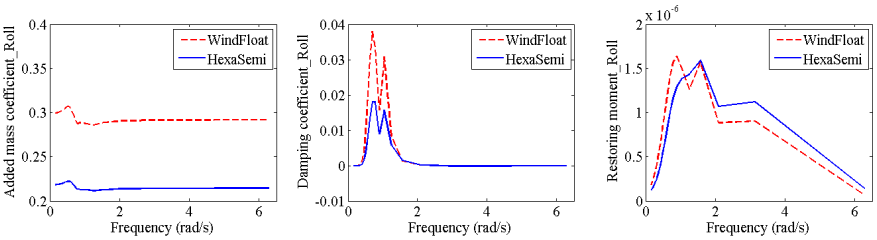

(**d**)

Figure 4. *Cont.*

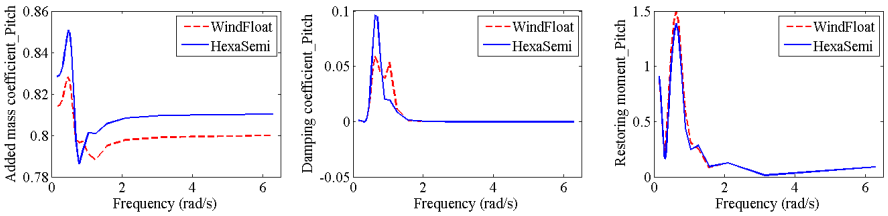

(**e**)

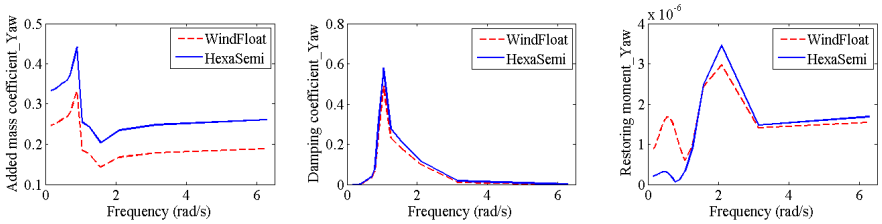

(**f**)

Figure 4. The comparisons of hydrodynamic coefficients in all six DOFs: (**a**) surge, (**b**) sway, (**c**) heave, (**d**) roll, (**e**) pitch, (**f**) yaw.

2.3. FAST

FAST (Fatigue, Aerodynamics, Structures, and Turbulence, version 8.16) is an aerodynamic-hydrodynamic-servo-elastic fully coupled simulation system developed by the National Renewable Energy Laboratory (NREL) and widely used in the design and analysis of horizontal axis wind turbine.

When simulating the dynamic response of a FOWT system, two modules, AeroDyn and HydroDyn, are invoked in FAST. AeroDyn is used for the calculation of aerodynamic load, and it adopts the blade element momentum theory (BEM) and the generalized dynamic wake theory (GDW), and also considers the dynamic stall correction. HydroDyn is the hydrodynamic load calculation module. Based on the classical linearization theory in hydrodynamics, it can calculate the hydrodynamic time-domain response of the floating wind turbine and the force on the mooring system. The Airy Wave theory is used in the linear theory to establish the hydrodynamic model using the potential flow. Therefore, the nonlinear viscous damping will be ignored.

In addition, structural dynamics module is established with the multi-body dynamics method. The blades and the tower are seen as a flexible cantilever beam structure whose quality and stiffness distribute continuously. The nacelle and hub are deemed as rigid body structures with a certain quality and moment of inertia, and thus both rigid and flexible parts of the machine movement model and dynamics model of wind turbine is established. As the mooring catenary of the FOWT system is provided with restoring force by gravity, the quasi-static catenary mooring line, which is one of the MAP++ options, is also considered, herein. A deep discussion of the theory of FAST in offshore applications is provided by Jonkman [17,18].

3. Free-Decay Motion

3.1. Heave-Decay Motion Simulated by CFD

The main dimensions of the WindFloat-type platform and HexaSemi are given in Tables 1 and 2. It is worth to note that the heave plates of the two platforms have the same area in order to create a fair comparison. However, the total circumferences of the two heave plates are different, shown in Figure 5. For the WindFloat-type platform, the summation of three independent heave plates' circumferences is 281 m. While, as for the HexaSemi's integral heave plate, the summation of the outer circumference and the inner moonpool's circumference is 330.8 m. The total circumference of the HexaSemi's integral heave plate is 15.1% larger than those of the WindFloat-type platform.

Table 1. Main Parameters of the WindFloat-type platform-type platform.

Parameter	Value
Height of column (m)	33.600
Column diameter (m)	10.700
Thickness of heave plate (m)	0.030
Length of heave plate edge (m)	15.629
Column center to center (m)	56.400
Pontoon diameter (m)	2.200
Bracing diameter (m)	2.038
Operating draft (m)	22.900
Height of CG (m)	29.800
Height of buoyancy center (m)	10.904
Displacement/Tonnage (t)	7247.928
Moment of inertia about CG (kg·m^2)	[4.250 × 10^9, 4.250 × 10^9, 7.056 × 10^9]

Table 2. Main Parameters of HexaSemi.

Parameter	Value
Height of hexagonal prism (m)	33.600
Length of hexagonal prism edge (m)	5.884
Thickness of heave plate (m)	0.030
Length of heave plate edge (m)	8.771
Breadth of heave plate (m)	10.228
Prism center to center (m)	56.400
Breadth of pontoon (m)	2.000
Height of pontoon (m)	3.000
Operating draft (m)	22.900
Height of CG (m)	29.800
Height of buoyancy center (m)	11.377
Displacement/Tonnage (t)	7247.894
Moment of inertia about CG (kg·m^2)	[4.250 × 10^9, 4.250 × 10^9, 7.056 × 10^9]

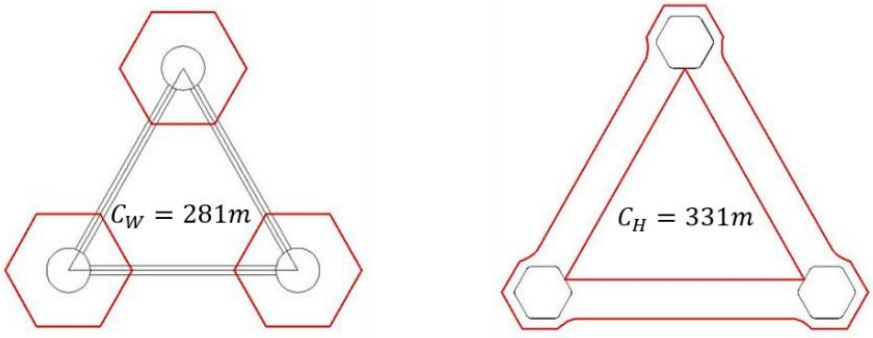

Figure 5. The total circumferences of (**a**) WindFloat-type platform and (**b**) HexaSemi.

The difference between the WindFloat-type platform and HexaSemi is only the heave plates' circumference and it is easy for the sharp edges of the heave plate to cause a large amount of vortex shedding, which is a form of energy transfer between the platform and the surrounding fluid. Figure 6 illustrates two transient vorticity diagrams during the heave-decay motion simulation of two platforms. It can be observed that there is more vortex shedding around the sharp edges of HexaSemi's integral heave plate when the platform moves up and down. The vortices represent high energy concentration. Therefore, the longer edge of HexaSemi's integral heave plate can dissipate more energy.

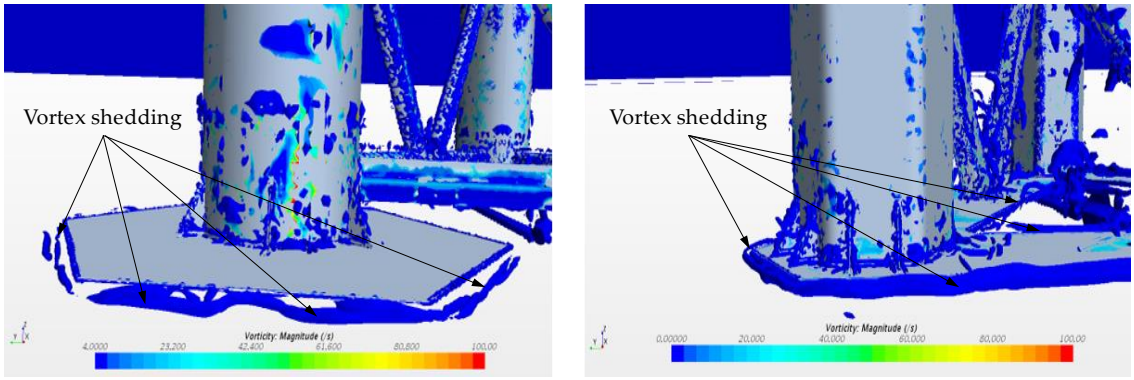

Figure 6. The vorticity of (**a**) WindFloat-type platform and (**b**) HexaSemi.

In the simulation, the initial heave displacement is chosen to be 1.5 m. Figure 7 presents a comparison of the heave-decay motion of the WindFloat-type platform and HexaSemi platform. It is found that the HexaSemi decays faster and heaves with a shorter period. Based on the time histories and the standard logarithmic procedure summarized by Mohsin et al. [19], the total damping coefficients of two platforms are given in Table 3. It has been noticed that the heave damping of the HexaSemi is larger than that of the WindFloat-type platform, and it agrees with the comparison of heave damping coefficient in Figure 4.

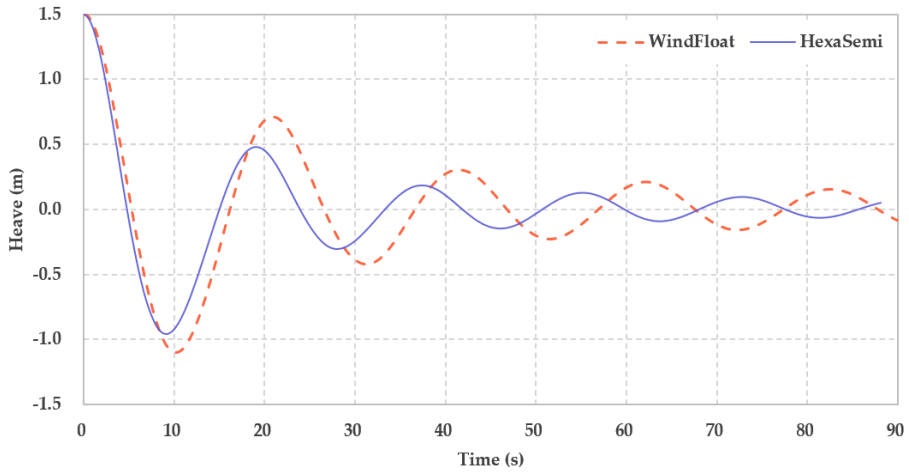

Figure 7. Free decay curves of heaving (WindFloat-type platform and HexaSemi).

Table 3. Total linear and quadratic heave damping of the two platforms.

Damping	WindFloat-Type	HexaSemi
Total linear heave damping (N/(m/s))	4.289×10^5	9.126×10^5
Total quadratic heave damping (N/(m/s)^2)	1.242×10^7	1.295×10^7

On the other hand, from a quantitative point of view, we calculate the attenuation rates of two platforms in the first three periods according to their free decay curves of heaving (see Figure 7). At first, the initial height and maximum height of the first three periods are selected. Then, the attenuation rates are able to be obtained, with the maximum height of each period dividing the initial height, respectively. Finally, the results are presented in Table 4. The first attenuation rate of the WindFloat-type platform and HexaSemi are 52.7% and 68.0%. It is noticed that the difference of the attenuation rate in the first period is 15.3%, which is consistent with the difference of the heave plates' circumference (the length of the outer and inner circumference of HexaSemi's integral heave plate is 15.1% larger than those

of the WindFloat-type platform). Therefore, the longer shaping edge of heave plates can dissipate more energy.

Table 4. The attenuation rate of heave free decay curves of the two platforms.

	Initial Height (m)	1st Period(m)	2nd Period(m)	3rd Period(m)
WindFloat-type	1.50	0.71	0.30	0.21
Attenuation rate 1		**52.7%**	80.0%	86.0%
HexaSemi	1.50	0.48	0.18	0.13
Attenuation rate 2		**68.0%**	88.0%	91.3%

3.2. Heave-Decay Motion Simulated by FAST

As mentioned previously, additional heave damping needs to be applied in FAST to imitate the viscous effects on the heave plate. By tuning the additional linear and quadratic damping coefficients, which are the input parameters in FAST, we achieve a close agreement between the CFD and FAST result for two platforms, as shown in Figure 8.

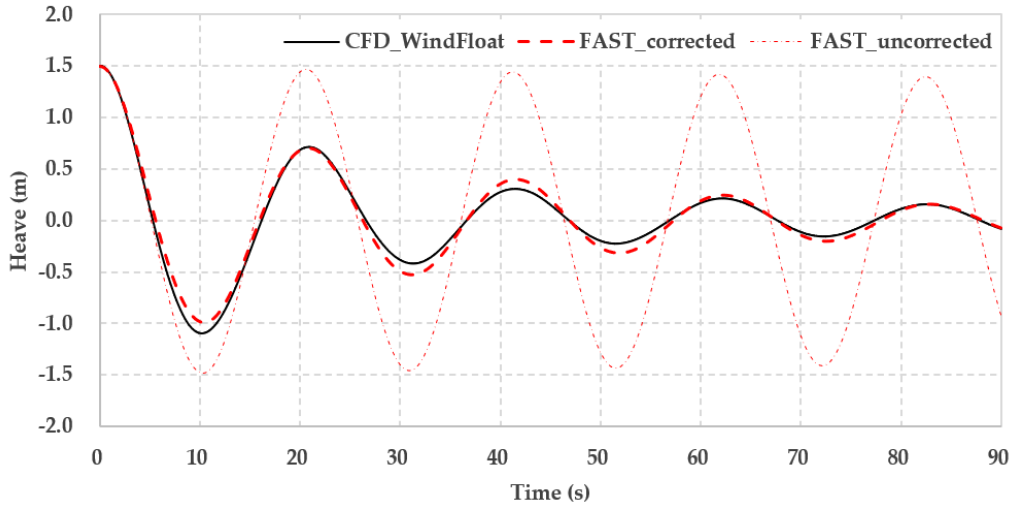

(**a**)

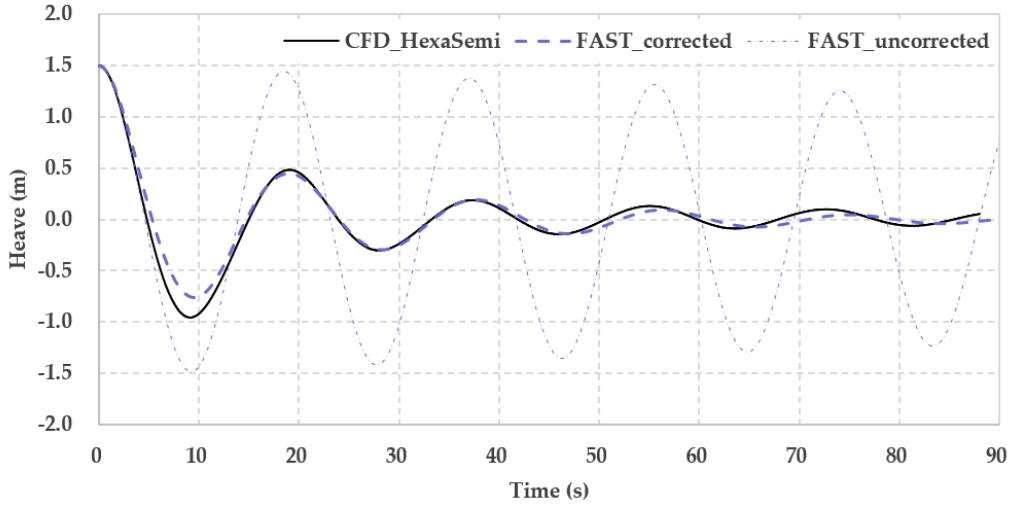

(**b**)

Figure 8. Three heave-decay simulations of (**a**) the WindFloat-type platform and (**b**) HexaSemi.

Table 5 gives the tuned additional linear and quadratic heave damping coefficients used in the following simulations. For the pitch and roll motion, we conduct the same CFD simulations for both platforms in order to implement the nonlinear pitch and roll damping coefficients into the FAST model. The results are also listed in Table 5.

Table 5. Additional linear and quadratic heave damping of the two platforms.

DOFs	Damping	WindFloat-Type	HexaSemi
Heave	Additional linear damping (N/(m/s))	1.08×10^6	9.65×10^5
	Additional quadratic damping (N/(m/s)^2)	4.23×10^6	4.20×10^6
Pitch	Additional linear damping (N·m/(rad/s))	2.41×10^9	1.80×10^9
	Additional quadratic damping (N·m /(rad/s)^2)	3.20×10^9	3.00×10^9
Roll	Additional linear damping (N·m/(rad/s))	2.39×10^9	2.70×10^9
	Additional quadratic damping (N·m /(rad/s)^2)	5.81×10^9	5.92×10^9

4. Motion Response under Different States

In this section, two load cases including an operational condition and a storm condition in the South China Sea are considered. Table 6 expounds on the load parameters in detail. The motion responses of the WindFloat-type platform and HexaSemi wind turbine system under two cases are simulated using the presented FAST code. The spectra and statistics of the 6-DOFs motion responses are investigated.

Table 6. Specific parameters of the two load cases.

Sea State	Irregular Wave		Turbulent Wind
	Hs (m)	Tp (s)	V (m/s)
Operational condition	7.45	13.60	14.54
Storm condition	15.18	16.96	34.40

4.1. Motion Response under an Operational Condition

The chosen time series corresponds to an operational condition described by a JONSWAP spectrum with significant wave height of 7.45 m, and mean wave period of 13.60 s, acting on the platform for duration of near 3 h (9999 s). The mean wind speed is 14.54 m/s with cut-in speed 3 m/s and cut-out speed 25 m/s of the NREL 5MW wind turbine. With regard to the control strategy, the variable rotor speed, adjustable pitch angle, and yaw system of nacelle has been turned on. Moreover, the encounter direction was zero degrees with respect to the x-axis, which is parallel to the platform surge direction, as shown in Figure 9.

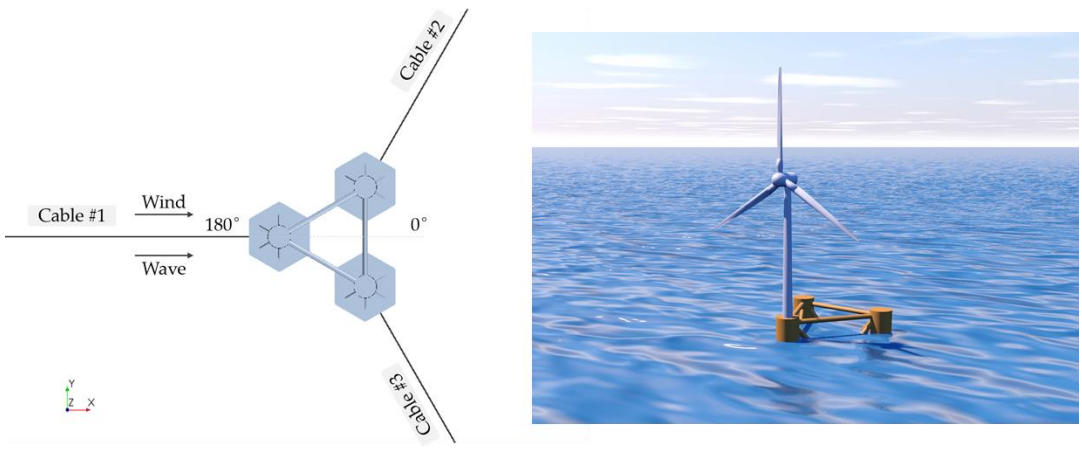

Figure 9. Illustration of the mooring system (**left**) and panorama of FOWT (**right**).

The WindFloat-type platform and HexaSemi are moored by three cables. The quasi-static catenary mooring line, which is one of the mooring analysis program (MAP) options, is considered herein. The mooring line properties are listed in Table 7.

Table 7. Mooring line properties.

Parameter	Value
Diameter of line (mm)	76.6
Mass density (kg·m^{-1})	126.5
Extensional stiffness (kN)	5.45×10^5
Fairlead to foundation center/ (m)	37.72
Fairlead below water surface (m)	10
Anchor below water surface (m)	200
Anchor to foundation center (m)	834.27
Unstretched mooring line length (m)	835.35

The time history curves of the two wind turbine systems' 6-DOF motions during the last 1000 s of the operational condition are given in Figure 10. To evaluate motion responses of the WindFloat-type platform and HexaSemi more intuitively, they are expressed in terms of a significant height as a representative value. The definition of significant response is similar to that of significant height in wave theory. Firstly, the 6-DOFs motion responses in time domain can be obtained by the simulation in FAST. Then, the time-domain motion response is sorted in descending order. Finally, the significant response is equal to the average of the 1/3 highest responses. The units we used for comparison are meter (m) for translational motions such as surge, sway, and heave, and degree (°) for rotational motions such as roll, pitch, and yaw. The statistical results during the last 2.5 h (9000 s) of FAST simulation are shown in Figure 11.

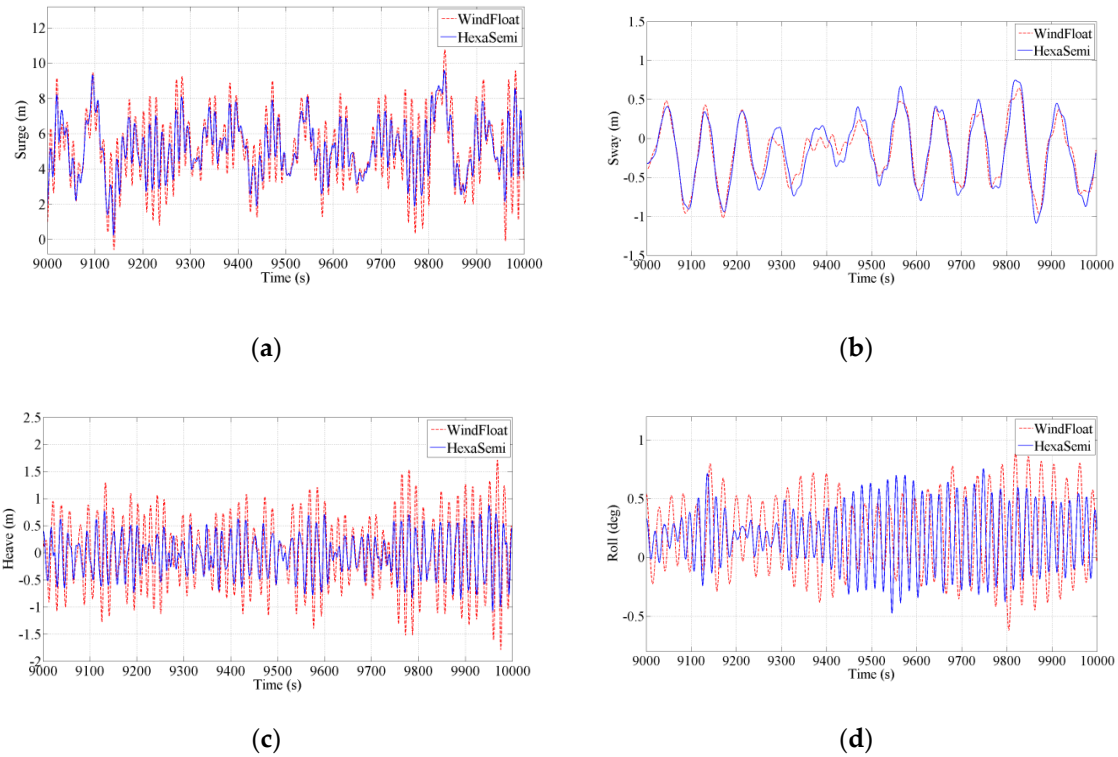

Figure 10. *Cont.*

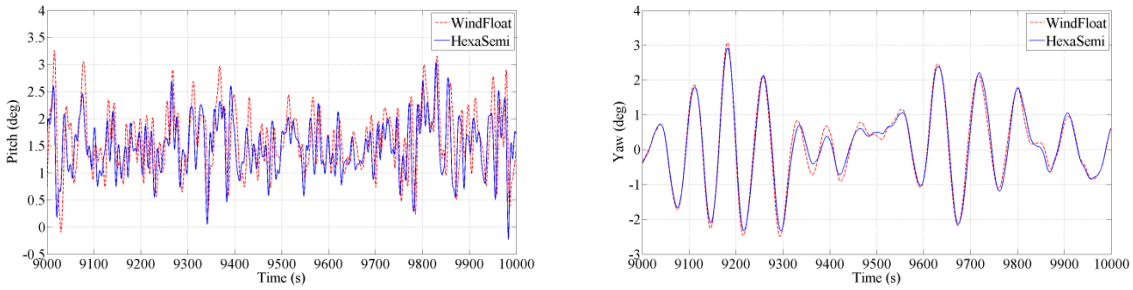

(**e**) (**f**)

Figure 10. 6-DOFs motion response under the operational condition: (**a**) surge, (**b**) sway, (**c**) heave, (**d**) roll, (**e**) pitch, (**f**) yaw.

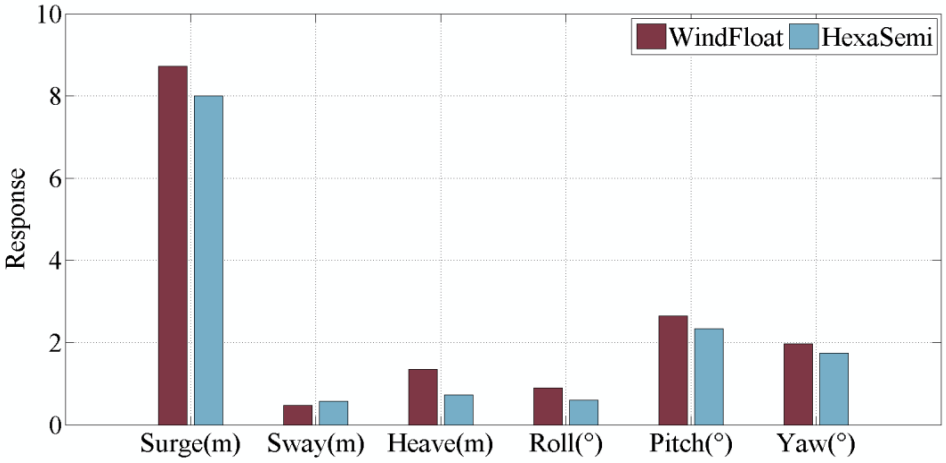

Figure 11. Comparison of 6-DOFs significant responses between the WindFloat-type platform and HexaSemi under the operational condition.

Overall, the differences in the motion amplitudes are significant, especially for the vertical-plane motions, which directly encounter the wave and wind loads in the simulated sea-state. It can be seen that the HexaSemi system sways slightly more in the last 1000 s of the simulation. However, it performs smaller motion amplitudes in the other five DOFs than the WindFloat-type platform. With respect to the surge and pitch motions, the two platforms with the rated-speed rotors (12.1 rpm) have an obvious drift, which is caused by the strong turbulent wind, providing a huge thrust force at the tower top.

In order to reveal the characters of the two platforms from a frequency perspective, we calculate the motion spectra of the 6-DOF motion, as shown in Figure 12. Referring to the surge motion, it is found that the first peak shows up in the low frequency region (<0.1 rad/s), which is induced by the combination of aerodynamic excitation [20] and the hydrodynamics nonlinearities [21]. Figure 13 shows the comparison of the surge motion spectra between the case with wave and wind loads and the case with the wave load only. It can be seen that the magnitude of surge response under combined wind and wave excitations is about 5–7 times as much as that under only wave excitation, at a low-frequency regime. We can draw a conclusion that the low frequency response in surge spectrum is induced by the combination of aerodynamic loads and the hydrodynamics nonlinearities, but it is primarily aerodynamic excitation induced. Therefore, the WindFloat-type and HexaSemi platforms supporting the same NREL 5-MW wind turbine, have the similar surge motion response at the low-frequency range, as shown in Figure 12a. However, the second peak associated response of Hexasemi in the wave energy range of 0.3 rad/s to 0.7 rad/s is much smaller. The second peak of the sway spectrum is generated by the roll DOF for strong coupling effects between different motions. In addition, the most different is the heave motion, and the peaks of the WindFloat-type platform spectra are twice as those

of HexaSemi, which indicates that the WindFloat-type platform absorbs much more energy than HexaSemi and the HexaSemi's integral heave plate reduces the responses effectively.

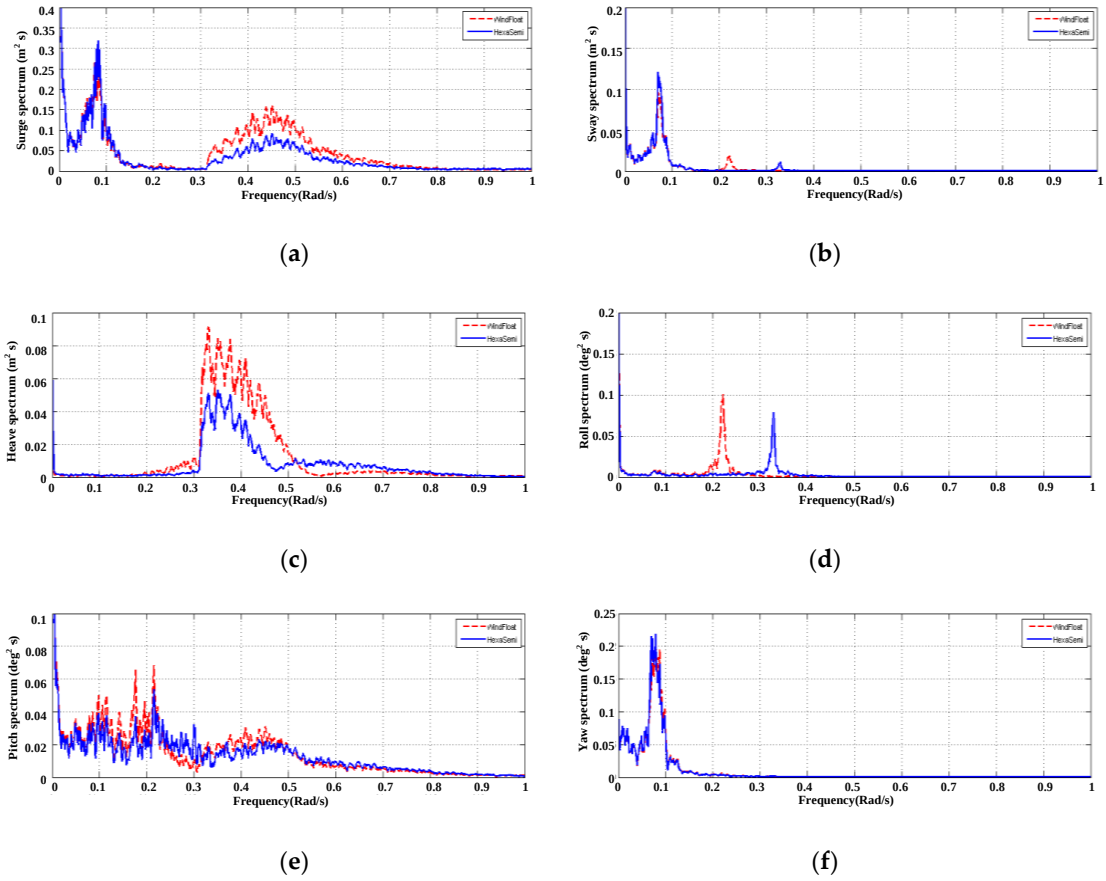

Figure 12. 6-DOFs motion spectrum under the operational condition: (**a**) surge, (**b**) sway, (**c**) heave, (**d**) roll, (**e**) pitch, (**f**) yaw.

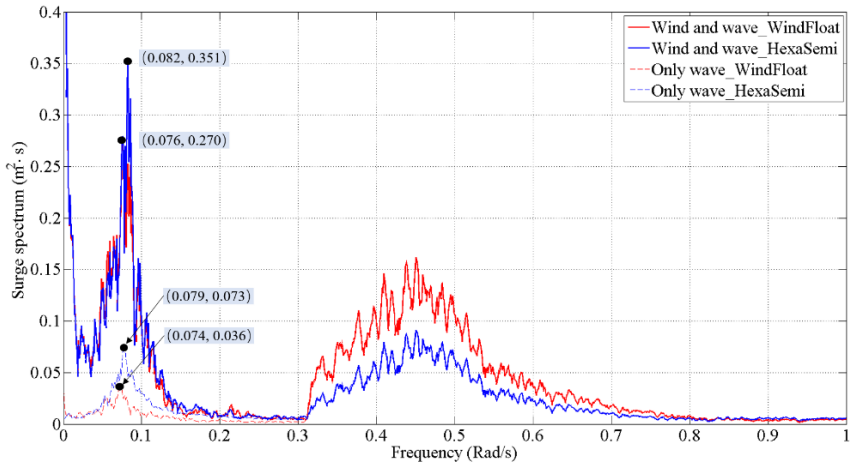

Figure 13. Comparison of surge spectrum under wind and wave induced condition and only wave induced condition.

Moreover, we find that the roll and pitch natural frequencies of the WindFloat-type platform are lower. This is because the outer ring of the single integral heave plate has a much larger diameter than that of the three independent heave plates. Vortex shedding at a larger diameter causes a larger hydrodynamic added moment of inertia. In fact, from a design perspective, larger roll and pitch

added moments of inertia are preferable because they can increase the corresponding natural periods, shift the incident wave period, and reduce the motion responses. However, based on the results shown in Figure 12, the roll and pitch spectra of the WindFloat-type platform design still have larger peaks. The natural periods of roll and pitch of HexaSemi are smaller and closer to the wave period of operational sea state (13.60 s), which may cause a larger response. However, the roll and pitch spectra of HexaSemi have lower peaks. It means that the integral heave plate helps dissipate more energy to the surrounding fluid.

4.2. Motion Response under A Storm Condition

The other case, also run for 9999s, is that FOWT with a locked rotor is under irregular wave with significant wave height of 15.18 m and mean wave period of 16.96 s, and the average turbulent wind speed of 34.40 m/s in South China Sea. The encounter direction and the mooring system is the same as the last section.

For the particular loading scenario, responses associated with surge, heave, and pitch motion receive the most excitation. As such, the 6-DOF motion responses of two wind turbine systems during the last 1000 s of the storm condition are shown in Figure 14.

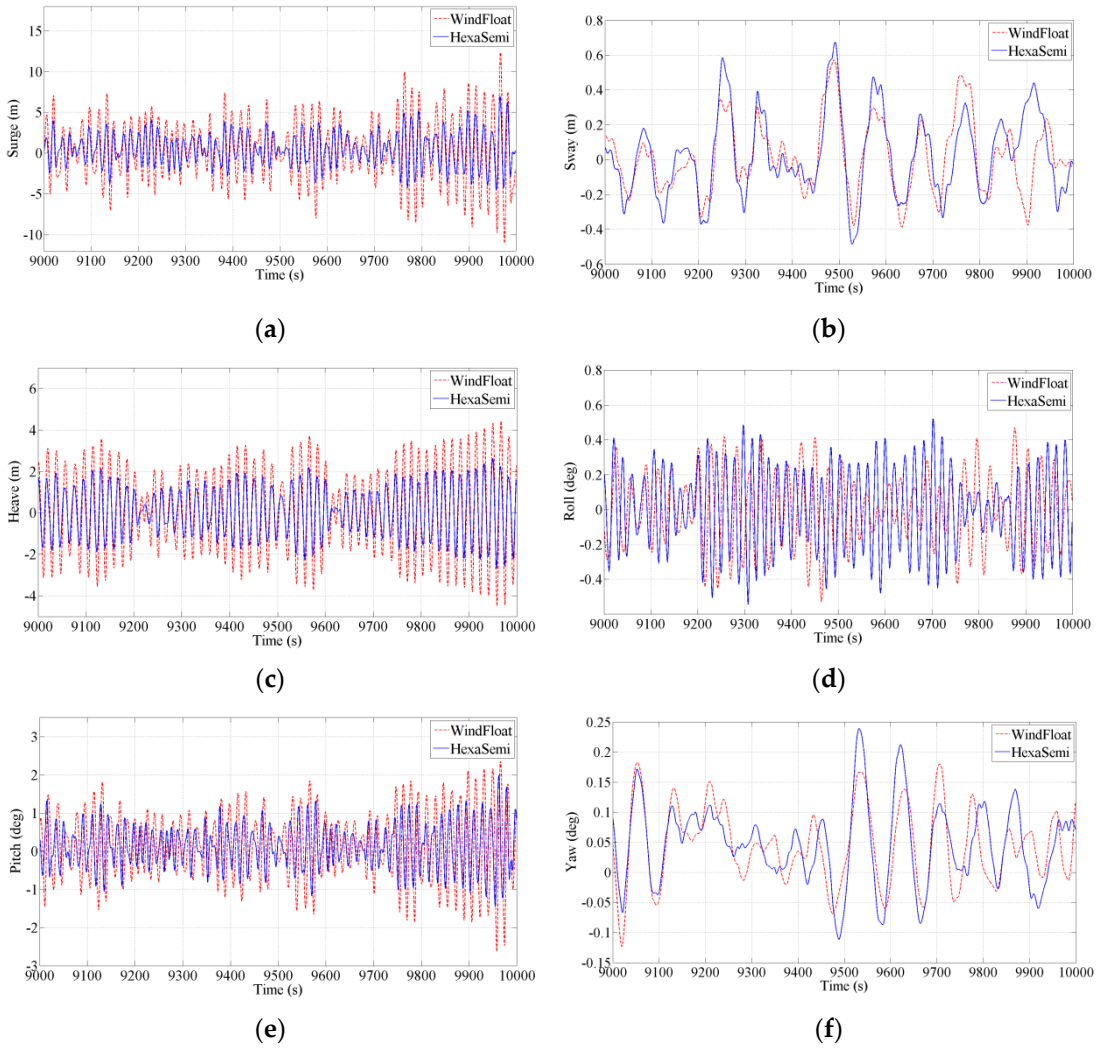

Figure 14. 6-DOFs motion response under the storm condition: (**a**) surge, (**b**) sway, (**c**) heave, (**d**) roll, (**e**) pitch, (**f**) yaw.

The significant height statistical results of FAST simulation under a storm condition are described in Figure 15. As can be seen in the figure, one obvious trend is that HexaSemi has smaller motion responses in surge, heave, and pitch in terms of the response amplitudes, though the responses of the other three DOFs seem to agree between these two wind turbine systems. Unlike the operational sea state, the equilibrium position of the surge motion response is near zero under the aforementioned condition with a storm. The reason for this is that the thrust load on the rotor and aerodynamic drag loads on the tower is low when FOWT encounters a storm sea state with a locked rotor and blade initial pitch angle is 90 degrees.

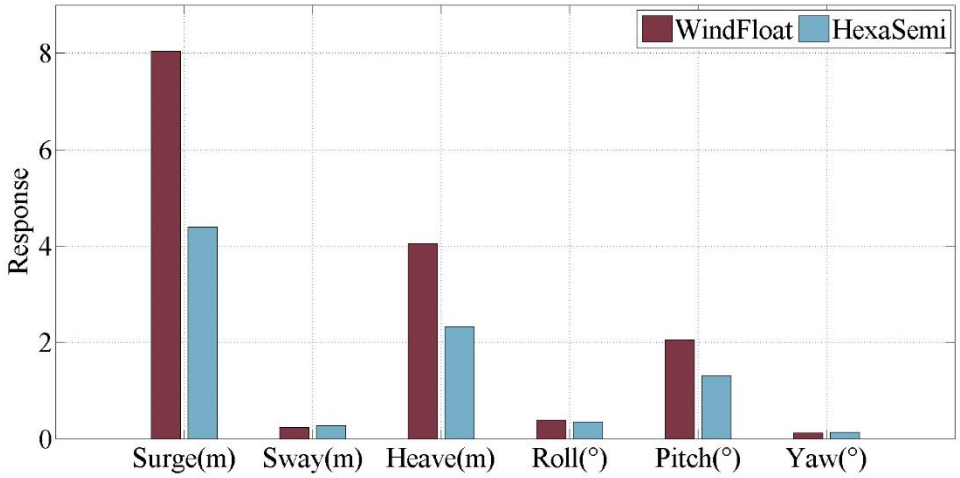

Figure 15. Comparison of 6-DOFs significant responses between the WindFloat-type platform and HexaSemi under a storm condition.

To further assess the hydrodynamics abilities of the two platforms, their motion spectrum comparisons are presented in Figure 16. Firstly, it is obviously noted that the surge, heave, and pitch motions of the WindFloat-type platform platform absorb much more energy than HexaSemi. The peaks of the WindFloat-type platform spectra are twice those of HexaSemi. This clearly reveals that the HexaSemi's integral heave plate dissipates more energy into the surrounding fluid, and helps reduce the motion responses. In addition, the sway and yaw motion spectrums of the two platforms appear to be the same and their values are very small because the waves we used for numerical simulation were only heading to sea. Therefore, we were able to neglect sway and roll motions under a storm condition.

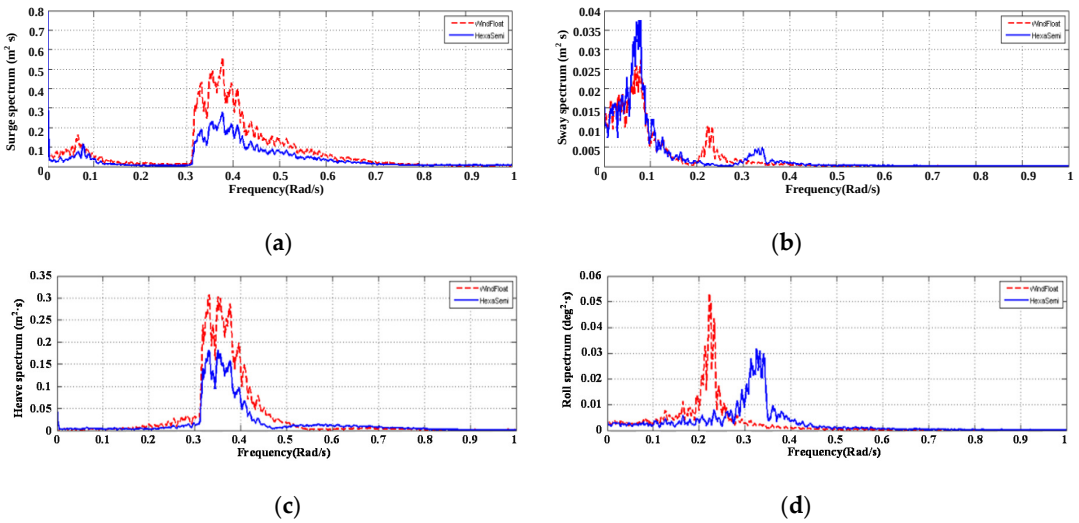

Figure 16. *Cont.*

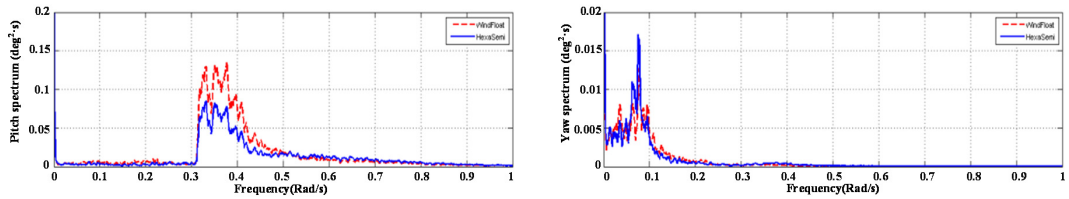

(**e**) (**f**)

Figure 16. 6-DOFs motion spectrum under the storm condition: (**a**) surge, (**b**) sway, (**c**) heave, (**d**) roll, (**e**) pitch, (**f**) yaw.

As for motion statistics, Tables 8 and 9 provide the 6-DOF motion statistics of the WindFloat-type platform and HexaSemi, including the mean value, maximum, minimum, motion range (the difference between the maximum and the minimum), and standard deviation value.

Table 8. 6-DOF motion statistics of WindFloat-type platform under a storm condition.

	Surge (m)	Sway (m)	Heave (m)	Roll (deg)	Pitch (deg)	Yaw (deg)
Mean	0.1959	0.0078	0.0250	−0.0020	0.1035	0.0560
Max.	14.060	0.5896	5.6180	0.6938	3.7400	0.2855
Min.	−16.190	−0.8282	−5.4770	−0.8008	−3.4410	−0.1232
Range	*30.250*	1.4178	*11.095*	1.4946	*7.1810*	0.4087
Std.	4.1295	0.1843	2.1839	0.2157	1.0022	0.0624

Table 9. 6-DOF motion statistics of HexaSemi under a storm condition.

	Surge(m)	Sway(m)	Heave(m)	Roll(deg)	Pitch(deg)	Yaw(deg)
Mean	0.4334	0.0092	0.0306	−0.0021	0.1052	0.0553
Max.	7.7790	0.7056	3.3800	0.6250	2.3830	0.2762
Min.	−7.3880	−0.7509	−3.2020	−0.6032	−2.2180	−0.1134
Range	*15.167*	1.4565	*6.5820*	1.2282	*4.6010*	0.3896
Std.	2.0716	0.2200	1.2346	0.1945	0.6293	0.0674

It is found that the two platforms perform quite well during severe storm condition. The motion statistics are quite acceptable with consideration of the chosen significant wave height. With respect to the difference of the response level between the two platforms, HexaSemi demonstrates better performance, especially for the surge, heave, and pitch motions, shown as the italic and underline data in Tables 8 and 9. Compared with WindFloat-type platform, these 3-DOFs motion ranges of HexaSemi are reduced by more than 30%.

Under the storm condition, the capacity of mooring system should be taken seriously. The mooring line tension statistics are provided in Table 10. Compared with the WindFloat-type platform case, the standard deviation of the mooring tension of the HexaSemi was found to be reduced by 50%, 51%, and 51% for mooring cable #1, #2, and #3, respectively. With respect to the range of mooring cable stress, the values for the HexaSemi case are reduced by 54%, 51%, and 52% for these three cables, respectively. Here, the HexaSemi design shows its superiority to the WindFloat-type platform design in consideration of the mooring safety under the storm condition.

Table 10. Mooring cable tension statistics.

Model	**WindFloat-Type Platform**			**HexaSemi**		
Cable #	**1**	**2**	**3**	**1**	**2**	**3**
Mean(kN)	1313	1271	1271	1302	1262	1261
Max. (kN)	2620	1695	1700	1827	1443	1435
Min. (kN)	689	1047	1045	938	1123	1119
Range(kN)	1931	648	655	889	320	316
Std. (kN)	252	78	78	125	38	38

5. Conclusions

In this work, the HexaSemi, a new semi-submersible platform, was put forward with a new designed heave plate that has better hydrodynamics performance. To explain why the proposed novel platform design can improve efficiency and load performance, the differences of the linear and quadratic damping properties between WindFloat-type and Hexasemi platforms were evaluated based on computational fluid dynamic simulations. Next, a FAST model with the consideration of fluid viscosity effects was established to analyze the dynamic response of the new platform under storm and operational conditions. The time-domain responses, motion spectra, and mooring-tension statistics of these two platforms were compared. As per the numerical results, we obtain the following conclusions:

(1) Fluid viscosity strongly affects the total damping of the floating platform with heave plate. The viscous damping effects should be considered in FAST simulations for predicting the dynamic response of the floating offshore wind turbine system.

(2) The attenuation rate of heave free decay motion in the first period is about 15.3%, and the difference of the heave plates' circumference is 15.1%. They are approximate, which illustrates that the circumference of heave plate is strongly related to the attenuation rate in heave DOF.

(3) The integral heave plate of the HexaSemi generates larger hydrodynamic damping than the independent heave plates of the WindFloat-type platform, because the HexaSemi's integral heave plate has a longer shape edge, which causes a larger amount of flow separation and dissipates more energy into surrounding fluid.

(4) The low frequency response under specified operational condition in surge spectrum is induced by the combination of aerodynamic loads and hydrodynamics nonlinearities, but is primarily aerodynamic excitation induced.

(5) Compared with the WindFloat-type platform, heave and pitch motion responses of HexaSemi are reduced by more than 30% and the standard deviation of the mooring tension of the HexaSemi is reduced by 50%, especially under the storm condition. The smaller motion responses help to reduce the mooring tension. Moreover, this structural design with an integral heave plate, which has better hydrodynamic performance, could provide a reference for the engineering application of floating offshore wind turbines.

Author Contributions: Conceptualization, Y.J.; methodology, Z.Z., Y.J., and L.Z.; software, G.H. and G.J.; validation, G.H. and G.J.; formal analysis, G.H.; investigation, G.H.; resources, G.H.; data curation, G.H.; writing—original draft preparation, G.H.; writing—review and editing, G.H., G.J. and Y.J.; visualization, G.H.; supervision, Y.J. and L.Z.; project administration, Z.Z., L.Z. and Y.J.; funding acquisition, Z.Z., L.Z. and Y.J. All authors have read and agreed to the published version of the manuscript.

Funding: The present work is supported by the Qingdao National Laboratory for Marine Science and Technology (QNLM2016ORP0402); National Natural Science of China (Grant No. 52001043, 51639003, 51279030, 51709042); and the Fundamental Research Funds for the Central Universities (DUT2017TB05). The authors are sincerely grateful for their support.

Conflicts of Interest: The authors declare no conflict of interest.

References

1. Wan, D.C.; Cheng, P.; Huang, Y.; Ai, Y. Overview of Study on Aero- and Hydro-Dynamic Interaction for Floating Offshore Wind Turbines. *Chin. Q. Mech.* **2017**, *38*, 5–27.
2. Jeon, S.; Cho, Y.; Seo, M.; Cho, J.; Jeong, W. Dynamic response of floating substructure of spar-type offshore wind turbine with catenary mooring cables. *Ocean Eng.* **2013**, *72*, 356–364. [CrossRef]
3. Heronemus, W.E. Pollution-Free Energy from Offshore Winds. In Proceedings of the 8th Annual Conference and Exposition Marine Technology Society, Washington, DC, USA, 11–13 September 1972.
4. Zhu, L.; Lim, H.-C. Hydrodynamic characteristics of a separated heave plate mounted at a vertical circular cylinder. *Ocean Eng.* **2017**, *131*, 213–223. [CrossRef]
5. Philip, N.T.; Nallayarasu, S.; Bhattacharyya, S.K. *Damping Characteristics of Heave Plates Attached to Spar Hull*; ASME International: New York, NY, USA, 2012; pp. 249–260.

6. Han, R.; Hao, H.; Gao, L.; Liu, T.; Liu, F. Effects of damping plate on the damping of a semisubmersible platform in its natural period. *J. Harbin Eng. Univ.* **2018**, *39*, 831–836.
7. Yu, W.; Ding, Q.; Li, C.; Hao, W.X.; Zhou, H.J.; Zhang, K. Influence of Heave Plate on the Dynamic Response of aFloating Wind Turbine Platform. *J. Chin. Soc. Power Eng.* **2018**, *38*, 747–754.
8. An, S.; Faltinsen, O.M. An experimental and numerical study of heave added mass and damping of horizontally submerged and perforated rectangular plates. *J. Fluids Struct.* **2013**, *39*, 87–101. [CrossRef]
9. Tao, L.; Dray, D. Hydrodynamic performance of solid and porous heave plates. *Ocean Eng.* **2008**, *35*, 1006–1014. [CrossRef]
10. Ji, H.; Huang, G.; Fan, J. The forced oscillation tests on heave damping plates. *J. Shanghai Jiao Tong Univ.* **2003**, *37*, 977–980.
11. Tran, T.; Kim, D.-H. The coupled dynamic response computation for a semi-submersible platform of floating offshore wind turbine. *J. Wind. Eng. Ind. Aerodyn.* **2015**, *147*, 104–119. [CrossRef]
12. Lee, C.; Newman, J.; Kim, M.; Yue, D. The computation of second-order wave loads. In Proceedings of the 10th International Conference on Offshore Mechanics and Arctic Engineering, Stavanger, Norway, 23–28 June 1991; pp. 113–123.
13. Li, A.J.; Tang, B.Y.; Yeung, C.R.W. Effects of second-order difference-frequency wave forces on a new floating platform for an offshore wind turbine. *J. Renew. Sustain. Energy* **2014**, *6*, 033102. [CrossRef]
14. Shin, H.; Kim, B.; Dam, P.T.; Jung, K. Motion of OC4 5MW Semi-Submersible Offshore Wind Turbine in Irregular Waves. In Proceedings of the 2013 International Conference on Offshore Mechanics and Arctic Engineering, Nantes, France, 9–14 June 2013. [CrossRef]
15. Karimirad, M. Modeling aspects of a floating wind turbine for coupled wave–wind-induced dynamic analyses. *Renew. Energy* **2013**, *53*, 299–305. [CrossRef]
16. CD-Adapco. *User Guide STAR-CCM+ (Version 14.02.010-R8)*; CD-Adapco: Melville, NY, USA, 2019.
17. Jonkman, J.M.; Buhl, M.L., Jr. *FAST User's Guide*; Technical Report NREL/EL-500-38230; National Renewable Energy Laboratory: Golden, CO, USA, 2005.
18. Jonkman, B.J. *Turbsim User's Guide*; Version 1.50; Office of Scientific and Technical Information (OSTI): Oak Ridge, TN, USA, 2009.
19. Irkal, M.A.; Nallayarasu, S.; Bhattacharyya, S. CFD approach to roll damping of ship with bilge keel with experimental validation. *Appl. Ocean Res.* **2016**, *55*, 1–17. [CrossRef]
20. Roald, L.; Jonkman, J.M.; Robertson, A.; Chokani, N. The Effect of Second-order Hydrodynamics on Floating Offshore Wind Turbines. *Energy Procedia* **2013**, *35*, 253–264. [CrossRef]
21. Karimirad, M.; Moan, T. Wave- and Wind-Induced Dynamic Response of a Spar-Type Offshore Wind Turbine. *J. Waterw. Port Coast. Ocean Eng.* **2012**, *138*, 9–20. [CrossRef]